Brodogradnja Volume 76 Number 1 (2025) 76104

journal homepage: www.brodogradnja.fsb.hr

Brodogradnja

An International Journal of Naval Architecture and Ocean Engineering for Research and Development

Impact of control strategies for wind-assisted ships on energy consumption

Cem Guzelbulut[1,*], *Timoteo Badalotti*[2], *Katsuyuki Suzuki*[1]

[1] *Department of Systems Innovation, School of Engineering, The University of Tokyo, Japan*
[2] *Monohakobi Technology Institute, Tokyo, Japan*

ARTICLE INFO

Keywords:
Wind-assisted ship propulsion
Heading control
Course control
Ship speed control
Energy consumption

ABSTRACT

Wind-assisted ship propulsion is one of the solutions for reducing greenhouse gas emissions by generating additional thrust using renewable wind power. Various technologies utilizing wind power to generate thrust are being developed and adopted by the industry. In addition to the thrust, side forces are also generated as secondary outputs, and they significantly affect ship motion. Although many studies have been conducted on the effects of sails on ship dynamics and energy consumption, the impact of control strategies of wind-assisted ships on energy consumption has not been clearly identified. This study aimed to determine the bearings of different control strategies on ships in terms of motion and energy. When the heading control strategy is adopted, rotor sails can reduce energy consumption by up to 10%. However, course- and speed-controlled ships without any wind-assistance devices can reduce energy consumption by 15%, and a further reduction of up to 30% can be achieved through rotor sails depending on the wind direction. When the control of the rotor sails was changed from a stand-alone controller to a ship dynamics-integrated controller, the energy consumption can be reduced by approximately 1-2% for course- and speed-controlled ships.

1. Introduction

Most large cargo ships in operation today use fossil fuels, which significantly increases greenhouse gas emissions. Hence, the International Maritime Organization (IMO) introduced regulations to reduce of emissions. According to the last revision of these regulations [1], the aim was updated to achieve net-zero emissions by 2050.

Wind-assisted ship propulsion is one of the options that reduce the dependence on fossil fuel through renewable energy. Three main types of wind-assisted propulsion systems exist: rigid wind sails, rotor sails, and kites. The design, operation, economics and life-cycle aspects of each system to efficiently utilize wind power are still under development. Ouchi et al. [2] proposed a sail with a crescent-shaped airfoil as the main propulsor and conducted several simulations to predict its energetic performance. Another type of wind sailing systems is the rotor sails. Rotor sails, invented by Anton Flettner in 1920s and also known as Flettner rotors, generate lift and drag forces by rotating when they are exposed to winds according to the Magnus effect. Many

* Corresponding author.
E-mail address: cem@struct.t.u-tokyo.ac.jp

http://dx.doi.org/10.21278/brod76104

Received 8 August 2024; Received in revised form 18 October 2024; Accepted 25 November 2024;
Available online 29 November 2024
ISSN 0007-215X; eISSN 1845-5859

studies have been conducted to understand and improve the performance of rotor sails to reduce greenhouse gas emissions. Kwon et al. [3] conducted a parametric computational fluid dynamics study to understand the effects of the aspect ratio and the ratio of the disk diameter to the cylinder diameter on the generation of lift and drag forces and torque. In another study, Chen et al. [4] conducted wind tunnel experiments on two rotor sails and investigated the aerodynamics of the rotor sails depending on the spin ratio, main dimensions of the sail and Reynolds number. The total force generation characteristics of the two rotor sails changed significantly owing to the interaction between them depending on the apparent wind angle and spin ratio, especially when the rotors were aligned with the wind direction. Tillig and Ringsberg [5] considered rotor sail-assisted ships and evaluated their efficiencies by considering different rotor sail layouts and ship routes. Guzelbulut et al. [6] proposed a model-based framework to predict the performance of rigid wind and rotor sails. Zhang et al. [7] compared wind sail- and rotor sail-assisted ship propulsion technologies in terms of thrust generation mechanisms and evaluated them by integrating a nonlinear ship dynamic model into the control algorithms. In addition to the performance of a single rotor sail, the interaction between rotor sails was investigated through wind tunnel experiments by Bordogna et al. [8].

Ship-speed control, irrespective of the wind-assisted devices, can have different forms, whereby the ship speed can be either optimized or used as is. Whenever the ship route is fixed, and the sea states and weather conditions that are forecast to be encountered are, known a priori, a method to minimize energy consumption along the route can be devised. For example, Li et al. [9] performed particle swarm optimization to determine the optimal speed profile along the route, thereby justifying the commonly adopted strategy of decreasing speed in heavy seas. Taskar and Anderson [10] showed that up to 45% reduction in fuel consumption can be achieved by reducing the ship speed by 30% depending on the particular ship and environment. Zincir [11], investigated the effect of slow steaming considering not only environmental aspects but also fuel and operational expenses. The study observed that slow steaming is an effective action for reducing fuel consumption and total costs by up to 50.1% and 23.3%, respectively. Alternatively, for a given route and ship speed, Ma et al. [12], employing operational data for a very large crude carrier (VLCC), estimated the power savings that could have potentially been obtained by adopting four cambered hard sails, where the operational data determined the route, ship speed, encountered sea state and weather conditions. The hard-sail angle of attack was set as the angle maximizing thrust while maintaining the set course through an autopilot, and the ensuing power reduction was evaluated. Such an approach, that is, to taking the ship speed as a given, is useful when a comparison with the experimental data is required. Otherwise, considering the speed as a variable extends the optimization space. However, in such scenario, a thrust-maximization approach as adopted by Ma et al. [12] to set the optimal hard-sail angle of attack does not necessarily provide the lowest required propeller power for two key reasons: First, as Ma et al. [12] indicated and Kramer and Steen [13] investigated in detail, the hard sail itself results in indirect resistance because it produces a drift force that has to be compensated for by the rudder, which, in turn, generates additional resistance; second, an increase in thrust results in an increase in ship speed and hull resistance. These two reasons imply that the propulsion system as a whole should be considered as the object of optimization to reduce the overall required propeller power. In particular, both course and sail angle should be targeted for the net-power minimization and increased efficiency of hard sails. This is the subject of this investigation.

As a further example of such mutual effects, according to Ghorbani [14], the fixed-speed operations of wind-assisted ships achieved through controllable pitch propellers are more efficient than variable-speed fixed-pitch operations, which is an effect of the increase in hull resistance with ship speed.

Although the main function of a wind-propulsion system is to produce thrust, the generation of side forces is inevitable. During the voyage, thrust and side forces are generated depending on the apparent wind speed, direction, and manner in which the sails are controlled. Side forces cause the ship to deviate from the target route, and this deviation should be compensated for by controlling the rudder angle. Elger et al. [15] used several models to predict the drift, rudder angle, and corresponding forces using an equilibrium equation. Kim et al. [16] implemented a proportional-integral-derivative (PID) controller to determine the rudder angle based on heading control and investigated the effect of rudder rotational speed on ship speed. Similarly, Li et al. [17] considered a PID controller for a trimaran to counter the disturbances caused by oblique stern waves

by integrating a Maneuvering Modelling Group (MMG) model and computational fluid dynamics simulations. Yanru et al. [18] studied the optimal control strategies for managing frequently changing course and speed conditions. Yingjie et al. [19] implemented a line-of-sight algorithm with rudder control and investigated the control aspects of wind-assisted ships. Although many studies have been conducted on heading- and course-controlled wind-assisted ships, their focus has been on the accuracy of control systems, rather than the energy aspects of control strategies. According to Geertsma et al. [20], an integrated control approach to the propulsion and power systems of ships plays an important role in efficient operation based on a comprehensive review of mechanical, electrical, and hybrid propulsion and power systems.

In this study, a case study was conducted to understand the effects of control strategies on the energy performance of ships, to determine which controlling action is suitable for wind-assisted ships, and to quantify the improvement in ship dynamic and sail-integrated controller over a stand-alone controller. First, a ship dynamic model was created, and both heading and course control strategies were employed by the autopilot. Subsequently, wind-assisted devices were tested for both strategies to assess their effectiveness with a stand-alone sail control. Finally, a controller integrating wind-assisted device and ship dynamics was devised and implemented, demonstrating holistic control as the best option.

2. Methods

In this study, different control strategies for ships and rotor sails were employed using a ship dynamics model.

2.1 Ship dynamics modelling

The ship dynamics model used in this study was created considering two coordinate systems. An earth-fixed coordinate system ($x_0 - y_0 - z_0$) was used to calculate the position and the equations of motion were defined in the ship-fixed rotating and translating coordinate system ($x - y - z$) whose center is the mid-ship position, as shown in Fig. 1. The center of gravity is located at (x_G, 0, 0) in the ship-fixed coordinate system ($x - y - z$).

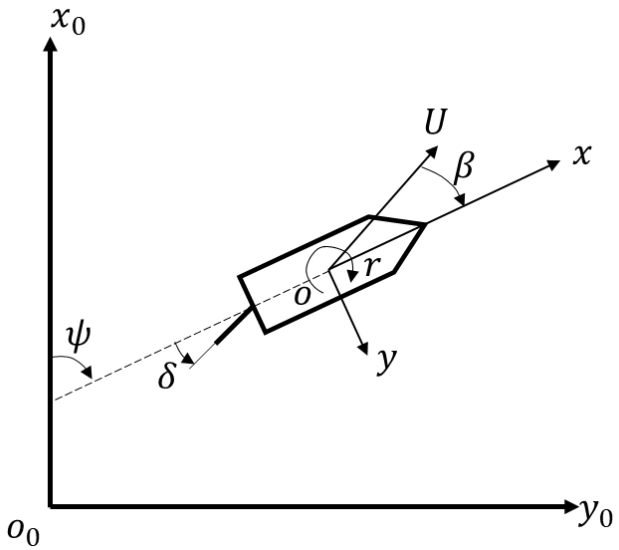

Fig. 1 Definition of earth reference frame and ship-fixed reference frame.

The ship dynamics were investigated based on the model developed by the MMG, as reported by Ogawa et al. [21] using three degrees-of-freedom: surge, sway and yaw [22]. Ship motion was calculated using Eq. (1), where m, m_x, m_y are the mass and added mass components in x- and y-directions, respectively; u, v_m and r are the surge, sway, and yaw velocity components of the mid-ship position, respectively; I_{zG} and J_z are the moments of inertia due to the mass and added mass according to the center of gravity, respectively; X, Y and N_m are the force and moment components in the x-, y-, and z-directions in the ship reference frame, respectively:

$$\begin{aligned}(m+m_x)\dot{u}-\left(m+m_y\right)v_m r-x_G m r^2 &= X\\ \left(m+m_y\right)\dot{v}_m+(m+m_x)ur+x_G m\dot{r} &= Y\\ (I_{zG}+x_G^2 m+J_z)\dot{r}+x_G m(\dot{v}_m+ur) &= N_m\end{aligned} \quad (1)$$

The total forces generated are broken down, as shown in Eq. (2), where the subscript *H* refers to the forces generated by hull hydrodynamics, *R* to rudder hydrodynamics, *P* to the propeller, *hull/wind* to hull-wind interaction, *hull/wave* to hull-wave interaction, and *sail* to the sail:

$$\begin{aligned}X &= X_H+X_R+X_P+X_{hull/wind}+X_{hull/wave}+X_{sail}\\ Y &= Y_H+Y_R+Y_P+Y_{hull/wind}+Y_{hull/wave}+Y_{sail}\\ N_m &= N_H+N_R+N_P+N_{hull/wind}+N_{hull/wave}+N_{sail}\end{aligned} \quad (2)$$

The target ship in this study was KVLCC2. The main particulars of the ship and height, H_{rotor}, diameter, D_{rotor}, and end plate diameter of the rotor sails, $D_{e,rotor}$, were given in Table 1. The length, breadth and draft of the ship are denoted by *L*, *B*, and *d*, respectively. The diameter of the propeller is denoted as D_P. The displacement volume of the ship is denoted by ∇. The position of the center of mass according to the ship-fixed reference frame at the mid-ship position is denoted by x_G. The area of the rudder is denoted as S_{rudder}. The block coefficient of the ship is denoted as C_B. The wind-assisted ship propulsion system used in this study was the rotor sails. The lift, drag and power characteristics of the rotor sails was determined using the prediction model described in previous studies [5,23].

Table 1 Main particulars of the KVLCC2. [24]

Parameters	Value	Parameters	Value	Parameters	Value
L (m)	320	∇ (m^3)	312600	H_{rotor} (m)	30
B (m)	58	x_G (m)	11.2	D_{rotor} (m)	5
d (m)	20.8	S_{rudder} (m^2)	112.5	$D_{e,rotor}$ (m)	10
D_P (m)	9.86	C_B	0.81		

The hydrodynamic forces, rudder force, propeller thrust, hull-wind and hull-wave interactions, and sail forces were determined using Eqs. (3-15). The hull hydrodynamics forces, X_H, Y_H, and N_H, were calculated using the hydrodynamic derivatives, X'_H, Y'_H, and N'_H, which were experimentally determined through polynomial regression as given in Eq. (3), where ρ is the density of water, L_{pp} is the ship length between perpendiculars, *d* is the draft, and *U* is resultant ship speed:

$$\begin{aligned}X_H &= (1/2)\rho L_{pp} d U^2 X'_{H(v'_m,r')}\\ Y_H &= (1/2)\rho L_{pp} d U^2 Y'_{H(v'_m,r')}\\ N_H &= (1/2)\rho L_{pp}^2 d U^2 N'_{H(v'_m,r')}\end{aligned} \quad (3)$$

Rudder forces were defined based on the interaction parameters (t_R, a_H and x_H), rudder normal force (F_N), and rudder angle (δ), as given in Eq. (4):

$$\begin{aligned}X_R &= -(1-t_R)F_N \sin\delta\\ Y_R &= -(1+a_H)F_N \cos\delta\\ N_R &= -(x_R+a_H x_H)F_N \cos\delta\end{aligned} \quad (4)$$

The propeller generates only thrust force in the *x*-direction as given in Eq. (5), which is determined by the thrust reduction factor (t_P), rotational speed (n_P), thrust coefficient (K_T):

$$\begin{aligned} X_P &= (1-t_P)\rho n_P^2 D_P^4 K_{T(J_P)} \\ Y_P &= 0 \\ N_P &= 0 \end{aligned} \tag{5}$$

Additionally, it requires a torque (Q), as given in Eq. (6), which is determined by the density of water (ρ), rotational speed (n_P), diameter of the propeller (D_P), and torque coefficient (K_Q):

$$Q = \rho n_p^2 D_P^5 K_{Q_{(J_P)}} \tag{6}$$

The coefficients of thrust and torque, K_T and K_Q, are defined as polynomial functions in Eqs. (7) and (8) with respect to advance ratio (J_P), which is defined in Eq. (9), where w_P denotes the wake coefficient:

$$K_T = k_0 + k_1 J_P + k_2 J_P^2 \tag{7}$$

$$K_Q = k_{q0} + k_{q1} J_P + k_{q2} J_P^2 \tag{8}$$

$$J_P = \frac{U(1-w_P)}{n_P \cdot D_P} \tag{9}$$

The polynomial coefficients are listed in Table 2. The variation in the wake coefficient depending on the geometric inflow angle (β_P), is defined in Eq. (10), where w_{P0} is the wake coefficient during straight motion ($\beta_P = 0$), and C_1 and C_2 are experimentally determined coefficients:

$$(1-w_P)/(1-w_{P0}) = 1 + (1-\exp(-C_1|\beta_P|))(C_2 - 1) \tag{10}$$

Table 2 Coefficients to describe the relation between J_P, K_T, and K_Q

Parameters	Value	Parameters	Value
k_0	0.2931	k_{q0}	0.03071
k_1	-0.2753	k_{q1}	-0.01856
k_2	-0.1385	k_{q2}	-0.02045

The forces owing to the environment such as the interaction between the hull and wind and between the hull and wave are calculated using in Eqs. (11) and (12) through non-dimensional parameters:

$$\begin{aligned} X_{Hull-Wind} &= (1/2)\rho_{air} A_F V_A^2 C_{XA(\theta_A)} \\ Y_{Hull-Wind} &= (1/2)\rho_{air} A_L V_A^2 C_{YA(\theta_A)} \\ N_{Hull-Wind} &= (1/2)\rho_{air} A_L L_{pp} V_A^2 C_{NA(\theta_A)} \end{aligned} \tag{11}$$

$$\begin{aligned} X_{Hull-Wave} &= \rho g H_{1/3}^2 L_{pp} \overline{C_{XW}}_{(U,T_v,\chi_0)} \\ Y_{Hull-Wave} &= \rho g H_{1/3}^2 L_{pp} \overline{C_{YW}}_{(T_v,\chi_0)} \\ N_{Hull-Wave} &= \rho g H_{1/3}^2 L_{pp}^2 \overline{C_{NW}}_{(T_v,\chi_0)} \end{aligned} \tag{12}$$

The interaction between hull and wind is defined using the density of air, (ρ_{air}), lateral and frontal projected areas of the ship above sea (A_L and A_F, respectively) apparent wind speed, (V_A), and force coefficients (C_{XA}, C_{YA}, and C_{NA}), which depend on the apparent wind direction (θ_A). The hull-wave interaction is defined based on the density of water (ρ), the gravitational acceleration (g), the significant wave height ($H_{1/3}$), and the wave force coefficients ($\overline{C_{XW}}$, $\overline{C_{YW}}$, $\overline{C_{NW}}$) which depend on ship speed (U), mean wave period (T_v), and direction (χ_0). The coefficients related to the interactions among the hull, wind, and waves were obtained from previous studies [25,26].

Another component is the rotor sails, as one of the wind sail systems, which generates lift (L), and drag (D), forces. L and D are given by the density of air, apparent wind speed (V_A), projected area (A), and the lift

and drag coefficients (c_L and c_D), which are functions of the spin ratio (SR), which is the ratio of the tangential speed of the rotor, given by the product of the rotational speed, (ω), and radius of rotor sail (R), to the inflow air speed (V_a), as shown in Eqs. (13)-(15):

$$\begin{aligned} L_{rotor} &= (1/2)\rho_{air} V_A^2 A c_{L_{(SR)}} \\ D_{rotor} &= (1/2)\rho_{air} V_A^2 A c_{D_{(SR)}} \end{aligned} \tag{13}$$

$$\begin{aligned} X_{sail} &= D\cos(\theta_A) - L\sin(\theta_A) \\ Y_{sail} &= D\sin(\theta_A) + L\cos(\theta_A) \\ N_{sail} &= Y_{WAD} \times x_{Sail} \end{aligned} \tag{14}$$

$$SR = \frac{\omega \times R}{V_a} \tag{15}$$

In this study, the fifth-order polynomial regression models used in a previous study conducted by Tillig and Ringsberg [5] were adopted to predict the lift and drag coefficients of the rotor sail, c_L and c_D, depending on SR. Subsequently, the generated lift and drag forces were transformed into the ship-fixed coordinate system.

Further details regarding the MMG model for wind-assisted ships can be obtained in published papers [6,27].

2.2 Control strategies for wind-assisted ships

For control of the ship movement, both heading and course control strategies were included in the study, as shown in Fig. 2. A route comprises a series of waypoints. Heading control involves turning the ship towards the next waypoint by rotating the rudder, thus mitigating drift forces and perturbations that would otherwise cause the ship to go off course. This strategy does not directly aim to minimize drift but to guarantee that the next waypoint is reached, which results in a curved trajectory in between waypoints. On the other hand, in the course control strategy, the ship follows a straight course between waypoints by fully counteracting the drift forces through the overcompensation of the heading angle, i.e., it turns beyond the angle at which it points to the next waypoint.

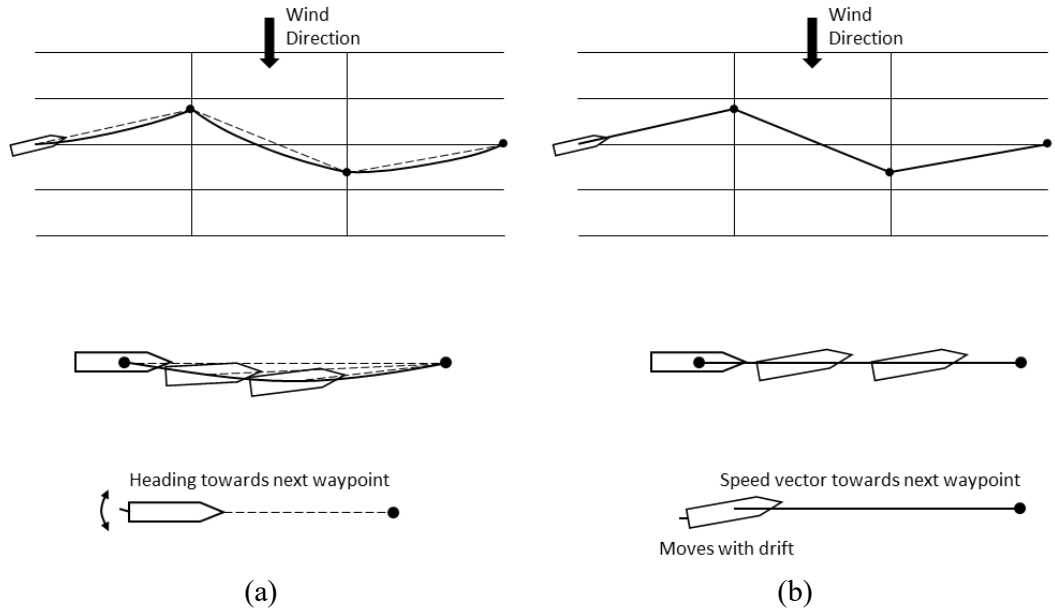

Fig. 2 Comparison of (a) heading and (b) course control strategies

Regarding wind assistance systems, many studies have focused on maximizing the net thrust power generated by the sails, discarding the generated side forces, which plays a major role in determining resistance.

Conversely, this study proposed and investigated a control strategy that integrates ship dynamics and sails by including the side forces acting on a ship. The five cases listed in Table 3 were considered.

Table 3 Description of the case study

	Ship	Ship control	Sail control
Case 1	No Sail	Heading Control, Fixed Propeller Revolution	-
Case 2	4 Rotor Sails	Heading Control, Fixed Propeller Revolution	Net Power Maximization
Case 3	No Sail	Course and Speed Controller	-
Case 4	4 Rotor Sails	Course and Speed Controller	Net Power Maximization
Case 5	4 Rotor Sails	Course and Speed Controller	Ship-Integrated Controller

2.2.1 Heading and Course Control

In the heading control strategy, the ship is assumed to navigate from one waypoint P_i to the next P_{i+1}. The difference between the ship heading ψ and the heading to the next waypoint ψ_f is calculated as heading error ψ_e, and the rudder angle is determined by feedbacking the heading error and using a PID controller, as shown in Fig. 3. In Cases 1 and 2, in which a heading controller is used, the rotational speed of the propeller is assumed to be constant. Voyage time changes with changing environmental conditions on the ship and sail, which results in differences in energy consumption.

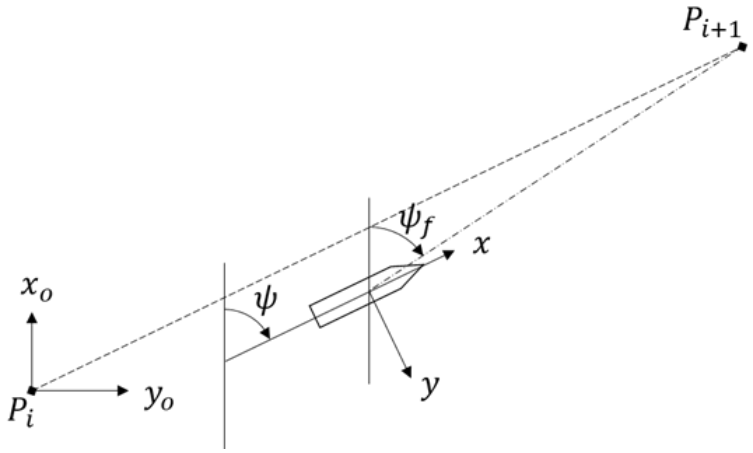

Fig. 3 Definitiion of heading error

In Cases 3, 4 and 5, the course and ship speed are controlled. As shown in Fig. 4, the ship navigates from P_i to P_{i+1}. A lead ship, which is indicated by the dashed line, follows a straight path between waypoints at a constant speed, and its position along the path is the position at time $t+T_{ref}$, where t is the current time and T_{ref} is the lag imposed to make it the leading ship. The lead ship can be on the next leg, that is the segment between the next pair of waypoints. The heading error (ψ_e) and speed error (u_e) are defined in Eqs. (16) and (17):

$$\psi_e = \psi - \text{atan}\left(\frac{y_{ref}-y}{x_{ref}-x}\right) \tag{16}$$

$$u_e = u - \frac{\sqrt{(x_{ref}-x)^2+(y_{ref}-y)^2}}{T_{ref}} \tag{17}$$

The rudder angle and propeller revolution rate are determined using PID controllers. The propeller revolutions change in response to different environmental conditions, thereby affecting the energy consumed. However, in contrast to the heading control strategy, the voyage time is roughly conserved.

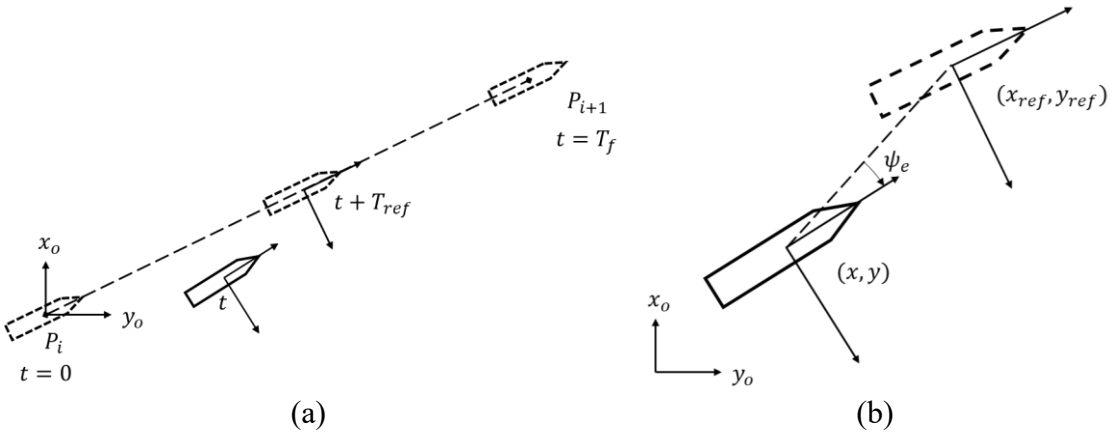

Fig. 4 Description of course and speed controlling strategy and (b) the close-up view between lead ship and real ship.

2.2.2 Control of rotor sails

The thrust and side forces generated by rotor sails depend on the spin ratio. Therefore, it is necessary to determine the spin ratio that minimizes the fuel consumption for a given wind speed and direction.

Two control strategies were considered in this study, as shown in Fig. 5. In the first method, only the thrust generated by the sails is considered and ship dynamics are not considered. In contrast, the second approach utilizes a surrogate model to predict the propeller power depending on the environment and spin ratio of the rotor sails, using the MMG model to include the ship dynamics to operate the rotor sails optimally.

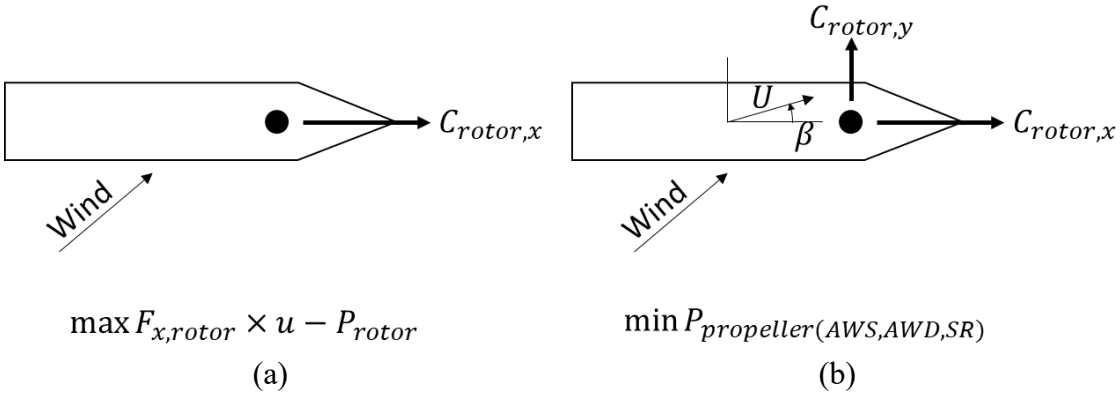

Fig. 5 Overview of (a) the thrust maximized control and (b) ship dynamics-integrated control of rotor sails.

The first method for determining *SR* maximizes the difference between the thrust power and power necessary to operate the rotor sail (P_{rotor}), as shown in Fig. 5, whereas the second method minimizes the power of the propeller. The first method is referred to as "net power maximization", where the objective of the optimization is to maximize the propulsive power by determining *SR*, whereas the second method is referred to as "ship-integrated controller".

To implement the latter approach, a model of propeller power as a function of *SR* for a ship travelling a straight course at a given apparent wind speed (*AWS*), and apparent wind direction (*AWD*) was created. To build the propeller power model, we conducted 456 simulations under the conditions listed in Table 4. Subsequently, *AWS* and *AWD* were calculated, and a fourth-order polynomial regression function was fitted to the simulation results to predict the propeller power, where the coefficients were determined using the least-squares method.

Table 4 Environmental conditions used in the simulation database of the power prediction model

Parameters	Datapoints
True wind speed, *TWS* (m/s)	[4.4, 9.8, 15.7, 22.7]
True wind direction, *TWD* (°)	[0, 10, 20, 30, …, 150, 160, 170, 180]
Spin ratio, *SR*	[0, 1, 2, 3, 4, 5]

3. Results

In Cases 1 and 2, a heading-controlled ship with a fixed propeller revolution was used to investigate the effect of sails on the ship dynamics and performance, as shown in Fig. 6. As the propeller revolution was kept constant, the additional thrust generated by the sails increased the ship speed from 7 to 8 m/s, which resulted in a change in the voyage time between the waypoints. In addition to the change in ship speed, the implementation of rotor sails on a heading-controlled ship increased the drift angle owing to generated side forces. When it comes to the energy aspects of having 4 rotor sails on heading controlled ships, rotor sails contributed to a reduction in voyage time by generating thrust forces and it can be concluded that the total reduction in energy by sails was approximately 8% at the maximum in heading control cases, under the environmental conditions of the Beaufort scale of 7 at different wind directions.

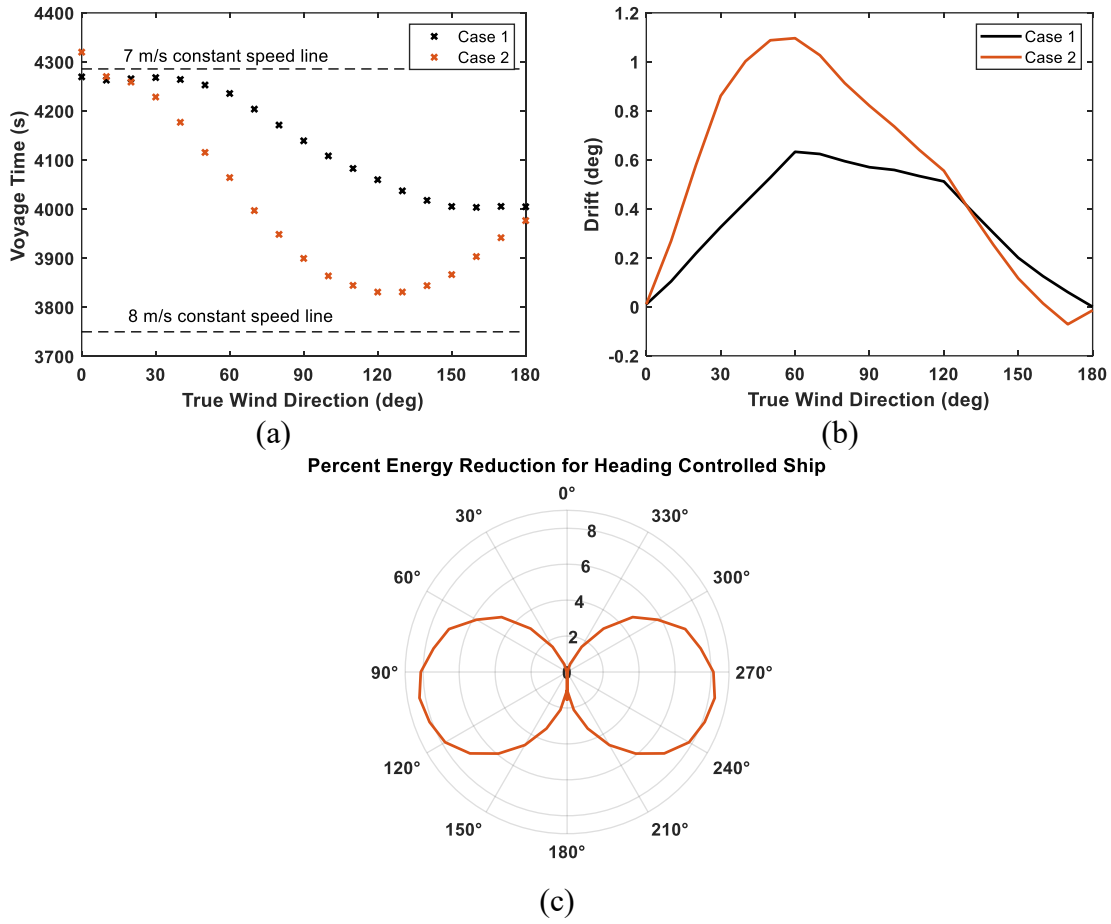

Fig. 6 Variation in (a) voyage time and (b) drift angle depending on the true wind direction with and without rotor sails, and (c) percent energy reduction achieved by rotor sails

However, the distance between waypoints can affect energy performance owing to divergence from a straight route. To examine the effect of the distance between waypoints, simulations were repeated by increasing the distance between waypoints from 30 to 100 km, and it was found that an increase in voyage length slightly reduced the drift angle and improved the effectiveness of rotor sails by contributing to the

reduction in energy consumption more than that achieved by a shorter distance between waypoints, as shown in Fig. 7.

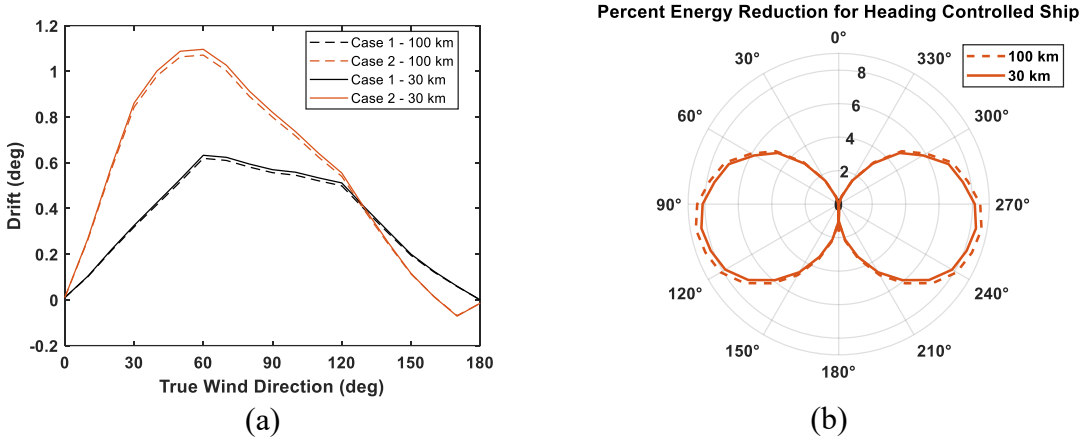

(a) (b)

Fig. 7 Effect of changing the distance between waypoints on (a) drift and (b) percent power reduction

When the heading-controlled ships (Cases 1 and 2) and course- and speed-controlled ships (Cases 3 and 4) were compared, regardless of whether rotor sails were adopted, the course- and speed-controlled ships exhibited slightly larger drift angles, as shown in Fig. 8. Moreover, the course- and speed-controlled ships, irrespective of the wind-assisted device used, consumed significantly less energy on average than the heading-controlled ships, thus demonstrating the paramount importance of a holistic control strategy. In addition, as expected, according to Fig. 8(b), the addition of wind-assisted devices further reduced the average power, resulting in a maximum reduction of 30% compared with the heading-controlled ships without any rotor sails, which was achieved with four rotor sails installed on a course- and speed-controlled ship.

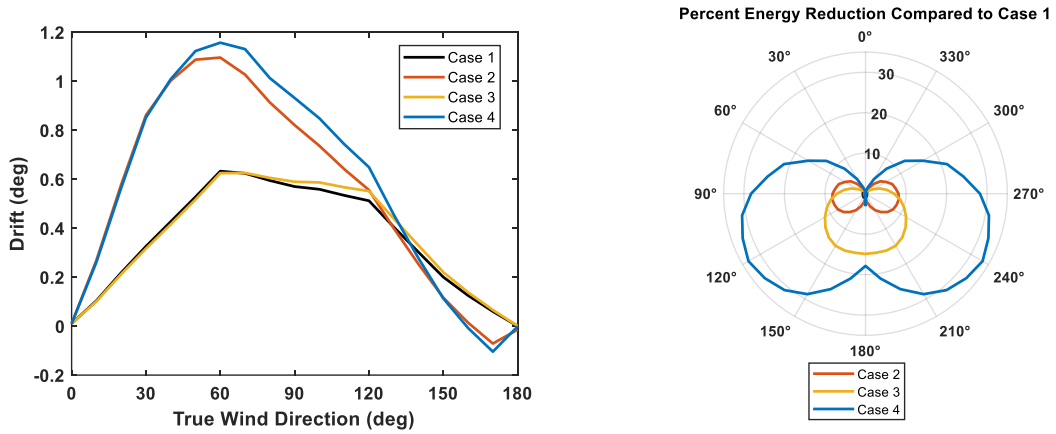

(a) (b)

Fig. 8 (a) Drift angle depending on true wind direction, control strategies, and rotor sails, and (b) reduction in energy consumption compared with heading controlled ships without any rotor sail.

In Case 5, the control strategy of the rotor sails was changed by considering the ship dynamics to improve their effectiveness. The spin ratio was determined by minimizing the propeller power at each time step using the average propeller power model described above, including the effects of side forces, drift, and resistance due to the sway speed, etc. Additionally, ship integrated controller for rotor sails mounted on a course- and speed-controlled ship slightly increased the drift angle for most of true wind directions, as shown in Fig. 9. When course- and speed-controlled ships without any rotor sails (Case 3) was considered as a reference, the installation of rotor sails with net power maximization strategy was observed to reduce energy consumption by up to 25%, and the energy consumption could be reduced further using ship integrated controller for rotor sails. The contribution of the ship integrated controller became clearer under the influence of side forces by further reducing the average energy consumption.

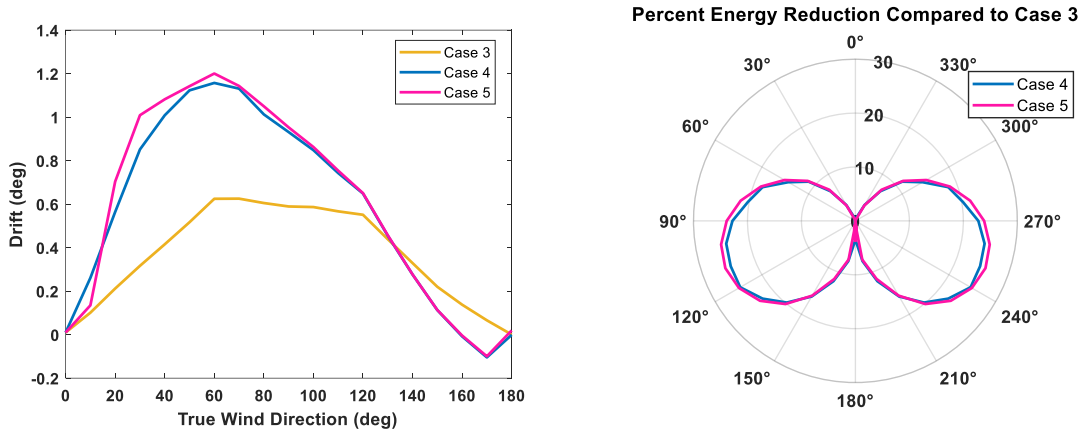

(a) (b)

Fig. 9 (a) Drift angle depending on the true wind direction and rotor sail control strategies, and (b) percent energy reduction depending on the sail control strategies.

4. Discussion

To date, studies have focused on the design and implementation of different wind-assisted propulsion technologies to utilize wind power as a secondary propulsion technology. However, the effects of the different propulsion technologies depend on their control. An investigation was conducted to identify how the control of a ship and its wind assisted devices affect its energy consumption. Two ship control strategies were considered: a heading controller with a fixed propeller revolution and a course- and speed-controller. For control of wind-assisted devices, a stand-alone controller that maximizes the thrust power generated by the sails and a ship dynamics-integrated controller were compared.

In Case 1, a heading-controlled ship without sails was investigated using fixed propeller revolutions. Depending on the wind direction, different side forces were generated, which caused divergence from a straight path. When the distance between the waypoints increased, the heading error became less sensitive, and a larger deviation from a straight route was expected. This reduced the aggressiveness of the control action, resulting in a reduced drift angle and lower fuel savings, as shown in Fig. 7. The same trend was observed when rotor sails were installed, as in Case 2. Furthermore, when wind sails were installed, at the same distance between waypoints, larger drift angles were observed owing to the larger side forces generated by the sails.

In Case 3, course- and speed-control was implemented for a ship without any sails. Unlike in Case 1, the ship followed a straight route, and an increase in the drift angle was generated to balance the side forces and yaw moment, as shown in Fig. 8. The increase in drift owing to the larger side forces was evident when the sails were installed, as in Case 4. For energy consumption, implementing a course- and speed-controller on the ship regardless of whether the ship was equipped with sails provide a greater contribution to the average power reduction than implementing four rotor sails on heading-controlled ship with fixed propeller revolutions. The main reason for this behaviour lies in the difference in the handling of the additional thrust or resistance, which occurred owing to varying environmental and operational conditions: controlling the ship speed with its course enables adjustments of the ship speed based on the position of the lead ship. However, pure heading control of wind-assisted ships keeps the propeller revolutions constant, thus resulting in an increase in ship speed due to the additional sail thrust. This increases the resistance and reduces the effectiveness of the sails. It should be noted that this study did not consider variations in engine efficiency due to engine speed. Moreover, the trade-off between engine efficiency and the number of rotor sails should be further investigated.

Another important problem in the control of wind-assisted ships is determining the rotational speed of rotor sails. The aerodynamics of rotor sails are typically characterized by their spin ratio. The main strategy for determining the spin ratio is to maximize the thrust power generated by the sail. However, rotor sails generate side forces, which affect ship dynamics and performance, in addition to thrust. In this study, a ship-

integrated controller was proposed to include the effects of ship dynamics. Ship-integrated control had a better operating point to minimize the average power although larger drift forces were generated. An integrated ship dynamics controller provides a prediction of how much power reduction can be achieved depending on the operating and environmental conditions instead of maximizing the sail thrust power directly.

In Case 5, integrating the course- and speed-control for navigation and using a ship integrated control strategy for the rotor sails proved to be the most energy-efficient solution. It is important to emphasize that such holistic control strategies can significantly reduce the energy consumption of ships by deploying each subsystem under the overall optimal operating condition instead of the optimal condition for each subsystem. In future studies, the simulation model will be extended to investigate the integration of the main engines, shaft generators, auxiliary engines, other power sources, sinks, and converters.

In addition to the energy aspects of different control strategies, it is also necessary to consider the operational aspects. The performance of the different control strategies depends on the accuracy and robustness of the sensing system. Less accurate speed and position data may cause improper propeller revolution, which may increase the ship speed and result in higher energy consumption. In addition, if the sensing system fails, the controller action may not be properly set. Thus, sensor fusion algorithms, such as Kalman filter, should be incorporated into the proposed control strategies in future studies to analyze and mitigate the risk of failure.

In this paper, various strategies for controlling ship motion and sail operation are discussed to understand the importance of control strategies for the energy consumption of wind-assisted ships. Although simulation-based results provide significant insights for predicting the potential benefits, it is necessary to validate the amount of savings through a component-wise validation or full-scale sea trials. In this regard, a recent study conducted by Thies and Ringsberg [28] compared sea trials and simulation predictions and revealed that sea trials contain larger uncertainties than models. Thus, a component-wise validation is necessary to validate the proposed approach in future studies.

This study had some limitations. First, the rolling effect owing to the side forces generated by the sails was not included. In future studies, the rolling motion and roll-related hydrodynamic force components will be included in the model to predict the resistive forces more accurately. Second, the interaction between the rotor sails was not considered in this study. In future studies, high-fidelity interaction models should be incorporated to understand the effects of different arrangements of the four sails would affect the energy consumption characteristics of wind-assisted ships.

5. Conclusions

The efficiency of wind-assisted ships depends significantly on the weather and sea conditions to which the ship is exposed during the voyage. Therefore, route optimization is important for wind-assisted ships. In this study, we focused on control strategies that aim to follow a given route with an unconstrained ship speed in terms of energy consumption. Heading control with a fixed propeller speed and course control with a ship speed controller with and without rotor sails were compared to identify the impact of ship motion control strategies. In addition to motion control strategies, the control of rotor sails was also analyzed considering a stand-alone rotor sail controller that maximizes the net power of sails and a ship dynamics-integrated controller that includes the effect of side forces, hull dynamics, and the resistance due to drift and rudder. The following conclusions were drawn:

- The heading control strategy enables a ship to deviate from the straight route between two waypoints and a smaller drift angle occurs compared with the course control strategy. Analogously, because the course control strategy does not allow deviations from the straight route, larger drift angles occur to compensate for the effects of the side forces.

- Course control with a fixed ship speed addresses environmental disturbances more effectively and uses wind-assisted propulsion systems as substitutes for propeller power. Therefore, the energy consumption is

reduced by up to 30% with four rotor sails, whereas heading control with a fixed propeller speed can reduce the energy consumption by up to 8%.

• When ship dynamics is integrated with the sail controller through a surrogate model, the operating point of the sails changes slightly, and the energy consumption can be further reduced by up to 1%-2%.

This study had several limitations. Energy consumption was evaluated using the propeller power, where engine efficiency was not considered. When the propeller speed is significantly reduced, the engine efficiency decreases, and the expected reduction in energy consumption may not be achieved. In future studies, not only the main engine but also other power system components, such as shaft generators, auxiliary engines, and battery systems. will be incorporated into the model to seek an optimal holistic control strategy for wind-assisted ships. It is worth mentioning that the presented results were obtained by considering the target ship KVLCC2. When the target ship and number of sails change, the improvement in each controller may exhibit different improvements in fuel consumption. The aerodynamic interactions between sails were not considered in this study. In future studies, we plan to include the interaction effects of sails and utilize them in a ship dynamics-integrated controller.

ACKNOWLEDGEMENTS

This research was supported by REDAS: Fundamental Research Developing Association for Shipbuilding and Offshore, the Shipbuilders' Association of Japan.

We would like to thank Maritime and Ocean Digital Engineering (MODE) Laboratory members at the University of Tokyo for their research advice.

REFERENCES

[1] IMO. Initial IMO Strategy on Reduction of GHG Emissions from Ships. https://www.imo.org/en/OurWork/Environment/Pages/Vision-and-level-of-ambition-of-the-Initial-IMO-Strategy.aspx. accessed 5th October 2023.

[2] Ouchi, K., Uzawa, K., Kanai, A., 2011. Huge hard wing sails for the propulsor of next generation sailing vessel. *Proceedings of the Second International Symposium on Marine Propulsors*, 15-17 June, Hamburg, Germany.

[3] Kwon, C.S., Yeon, S.M., Kim, Y.C. Kim, Y.G., Kim, Y.H., Kang, H.J., 2022, A parametric study for a Flettner rotor in standalone condition using CFD. *International Journal of Naval Architecture and Ocean Engineering*, 14, 100493. https://doi.org/10.1016/j.ijnaoe.2022.100493

[4] Chen, W., Wang, H., Liu, X., 2023. Experimental investigation of the aerodynamic performance of Flettner rotors for marine applications. *Ocean Engineering*, 281, 115006. https://doi.org/10.1016/j.oceaneng.2023.115006

[5] Tillig, F., Ringsberg, J.W., 2020. Design, operation and analysis of wind-assisted cargo ships. *Ocean Engineering*, 211, 107603. https://doi.org/10.1016/j.oceaneng.2020.107603

[6] Guzelbulut, C., Sugimoto, T., Fujita, Y., Suzuki, K., 2024. Investigation of the efficiency of wind-assisted systems using model-based design approach. *Journal of Marine Science and Technology*, 29, 387-403. https://doi.org/10.1007/s00773-024-00993-6

[7] Zhang, G., Li, J., Chang, T., Zhang, W., Song, L., 2025. Autonomous navigation and control for a sustainable vessel: A wind-assisted strategy. *Sustainable Horizons*, 13, 100117. https://doi.org/10.1016/j.horiz.2024.100117

[8] Bordogna, G., Muggiasca, S., Giappino, S., Belloli, M., Keuning, J.A., Huijsmans, R.H.M., 2020. The effects of the aerodynamic interaction on the performance of two Flettner rotors. *Journal of Wind Engineering and Industrial Aerodynamics*, 196, 104024. https://doi.org/10.1016/j.jweia.2019.104024

[9] Li, X., Gu, Y., Fan, X., Zou, K., Hou, X., 2023. An Optimization model for ship speed based on maneuvering control. *Journal of Marine Science and Engineering*, 11(1), 49. https://doi.org/10.3390/jmse11010049

[10] Taskar, B., Andersen, P., 2020. Benefit of speed reduction for ships in different weather conditions. *Transportation Research Part D: Transport and Environment*, 85, 102337. https://doi.org/10.1016/j.trd.2020.102337

[11] Zincir, B., 2023. Slow steaming application for short-sea shipping to comply with the CII regulation. *Brodogradnja*, 74(2), 21-38. https://doi.org/10.21278/brod74202

[12] Ma, R., Wang, Z., Wang, K., Zhao, H., Jiang, B., Liu, Y., Xing, H., Huang, L., 2023. Evaluation method for energy saving of sail-assisted ship based on wind resource analysis of typical route. *Journal of Marine Science and Engineering*, 11, 789. https://doi.org/10.3390/jmse11040789

[13] Kramer, J.V., Steen, S., 2022. Sail-induced resistance on a wind-powered cargo ship. *Ocean Engineering*, 261, 111688. https://doi.org/10.1016/j.oceaneng.2022.111688

[14] Ghorbani, M., Slaets, P., Lacet, J., 2023. A numerical simulation tool for a wind-assisted vessel verified with logged data at sea. *Ocean Engineering*, 290, 116319. https://doi.org/10.1016/j.oceaneng.2023.116319

[15] Elger, D.E., Bentin, M., Vahs, M., 2020. Comparison of different methods for predicting the drift angle and rudder resistance by wind propulsion systems on ships. *Ocean Engineering*, 217, 108152. https://doi.org/10.1016/j.oceaneng.2020.108152

[16] Kim, S.S., Kim, S.D., Kang, D., Lee, J.H., Lee, S.J., Jung, K.H., 2015. Study on variation in ship's forward speed under regular waves depending on rudder controller. *International Journal of Naval Architecture and Ocean Engineering*, 7(2), 364-374. https://doi.org/10.1515/ijnaoe-2015-0025

[17] Li, Y., Tang, Z., Gong, J., 2023. The effect of PID control scheme on the course-keeping of ship in oblique stern waves. *Brodogradnja*, 74(4), 155-178. https://doi.org/10.21278/brod74408

[18] Yanru, H., Xingya, Z., Liwen, H., Luping, X., Jinlai, L., 2024. Control method for the ship track and speed in curved channels. *Brodogradnja*, 75(3), 75307. https://doi.org/10.21278/brod75307

[19] Yingjie, D., Xianku, Z., Guoqing, Z., 2019. Fuzzy logic based speed optimization and path following control for sail-assisted ships. *Ocean Engineering*, 171,300-310. https://doi.org/10.1016/j.oceaneng.2018.11.006

[20] Geertsma, R.D., Negenborn, R.R., Visser, K., Hopman, J.J., 2017. Design and control of hybrid power and propulsion systems for smart ships: A review of developments. *Applied Energy*, 194, 30-54. https://doi.org/10.1016/j.apenergy.2017.02.060

[21] Ogawa, A., Koyama, T., Kijima, K., 1977. MMG report-I, on the mathematical model of ship manoeuvring. *Bulletin of Society of Naval Architects of Japan,* 575, 22–28.

[22] Yasukawa, H., Yoshimura, Y., 2015. Introduction of MMG standard method for ship maneuvering predictions. *Journal of Marine Science and Technology*, 20, 37–52. https://doi.org/10.1007/s00773-014-0293-y

[23] Li, D., Leer-Andersen, M., Allenstrom, B., 2012. Performance and vortex formation of Flettner rotors at high Reynolds numbers. *29th International Symposium on Naval Hydrodynamics*, 26-31 August, Gothenburg, Sweden.

[24] MOERI KVLCC2 geometry and conditions, SIMMAN 2008, FORCE Technology. http://www.simman2008.dk/KVLCC/KVLCC2/kvlcc2_geometry.html. accessed 19th October 2024.

[25] Yasukawa, H., Zaky, M., Yonemasu, I., Miyake, R., 2017. Effect of engine output on maneuverability of a VLCC in still water and adverse weather conditions. *Journal of Marine Science and Technology*, 22, 574–586. https://doi.org/10.1007/s00773-017-0435-0

[26] Fujiwara, T., Ueno, M., Nimura, T., 1998. Estimation of wind forces and moments acting on ships. *Journal of the Society of Naval Architects of Japan*, 183, 77–90. https://doi.org/10.2534/jjasnaoe1968.1998.77

[27] Guzelbulut, C., Suzuki, K., 2024. Optimal design of rotor sails based on environmental conditions and cost. *Journal of Marine Science and Engineering*, 12, 31. https://doi.org/10.3390/jmse12010031

[28] Thies, F., Ringsberg, J.W., 2024. Sea trials vs prediction by numerical models—Uncertainties in the measurements and prediction of WASP performance. *Journal of Ocean Engineering and Science*. https://doi.org/10.1016/j.joes.2024.05.001